Regular Paper

Autonomous Driving on Community Roads Using Small Mobility: Route Generation Using Trajectory Prediction and 2D TTC

Takumi Seita*, Shunsuke Michita*, Seiji Komiya*, and Toshihiro Wakita*

*Graduate School of Engineering, Kanagawa Institute of Technology, Japan
s2384004@cco.kanagawa-it.ac.jp

Abstract - Traffic accidents occur frequently on community roads where pedestrians and vehicles coexist, therefore safe and smooth autonomous driving is expected. Based on this situation, this paper proposes a path planning method for autonomous vehicles by extending the Velocity Obstacles algorithm (VO). VO is commonly used in mobile robotics. Three points were extended to apply the algorithm. The first point was to use 2D TTC to reduce unnecessary avoidance. It was decided that avoidance would not be performed if there is room for it based on the 2D TTC calculation of collision time. The second point established motion constraints by assuming avoidance is performed with steady-state circular motion because vehicles have more motion constraints than robots. The third point was to change the collision detection method from circle approximation. Considering the size and shape of the vehicle, it was decided to draw tangents from the four corners of the vehicle to the obstacle and combine them. Using the above algorithm, avoidance paths were generated and better performance than VO, DWA and risk potential method.

Keywords: Autonomous Mobility, Pedestrian prediction

1 INTRODUCTION

1.1 Background

In recent years, although the reduction of traffic accident fatalities has been decreasing, the decreasing trend of the number of traffic accidents on community roads has remained relatively low. According to data from the Ministry of Land, Infrastructure, Transport and Tourism, in 2021, there were approximately 80,000 traffic accidents on community roads, compared to approximately 220,000 accidents on arterial roads [1]. In terms of the reduction rate since 2004, arterial road accidents have decreased by about 70%, while community road accidents have decreased by about 60%. Therefore, in order to reduce traffic accidents on community roads as well as arterial roads, the realization of safe and efficient autonomous driving is desired.

However, community roads have distinct characteristics such as the lack of white lanes, pedestrians freely walking along various paths, and narrow road widths, making a significantly different traffic environment compared to arterial roads. Because there are numerous problems that differ from previous autonomous driving environment, it difficult to achieve autonomous driving on community roads.

1.2 Related Research

Autonomous navigation in complex environments like community roads has been extensively studied in the context of mobile robots. Various research has been conducted on obstacle avoidance methods for mobile robots.

The dynamic window approach (DWA) [2] is an approach that generates trajectory candidates by combining translational and rotational velocities. It evaluates each generated trajectory using an evaluation function. Following that, the trajectory with the highest evaluation value is selected, and the robot follows that trajectory. One of the problems of this method is that it does not consider dynamic obstacles, which may result in insufficient avoidance of dynamic obstacles such as pedestrians.

The risk potential method [3] defines repulsive potentials and an attractive potential to the target reaching position to obstacles. It generates target velocities and target paths based on the calculated potential gradients. One of the problems of this method is that the generated potential field is a virtual quantity without physical meaning. Due to the lack of physical significance, parameter adjustments are required, making it difficult to achieve proper control of the trajectory, velocity, and adaptation to various traffic environments.

The freezing robot problem (FRP) have focused on predicting the future actions of pedestrians using Social LSTM [4] and avoiding areas that may obstruct pedestrians (Potential Freezing Zone: PFZ) [5]. However, these methods address only pedestrians.

There is a VO algorithm [6] as a method to avoid various dynamic obstacles such as pedestrians, bicycles, and other vehicles. VO is a method for motion planning of a robot in a dynamic environment with moving obstacles. This method defines a "velocity obstacle" as the velocity space within which a robot may have potential collisions based on the current positions and velocities of the robot and obstacles. By calculating velocity obstacles for all obstacles and selecting a velocity that does not belong to any velocity obstacle, this method generates obstacle-avoiding trajectories. VO is considered suitable for path planning on community roads, as it is an effective method for avoiding dynamic obstacles.

Up to now, various extensions have been attempted in VO. Reciprocal Velocity Obstacles (RVO) [7] address the vibration problems that arise when VO robots need to avoid each other. Optimal Reciprocal Collision Avoidance (ORCA) [8] addresses the shortcomings of RVO, which only guarantees collision avoidance under specific conditions and does not provide a sufficient condition for general collision avoidance. This method presents sufficient conditions for multiple robots to avoid collisions with each other, ensuring collision-free navigation. Adaptive Velocity Obstacles (AVO) [9] is proposed to solve that if the robot chooses the critical velocity of the collision cone to minimize the time consumption, the error of the sensor will lead to the collision. Ellipse-based Velocity Obstacles (EBVO) [10] derived the VO for an elliptic robot, and showed that the robot could reach the goal with a less traveled path by controlling the rotary motion. As these extensions are not effective for path planning on community roads where it is necessary to avoid obstacles such as pedestrians and other vehicles, this study attempted to apply the original VO algorithm.

1.3 Research Question

VO is suited for mixed pedestrian and vehicular environments on community roads, but it originally developed for mobile robots. Consequently, adapting VO directly to vehicles in mixed pedestrian and vehicular environments on community roads appears several problems.

The first problem is the existence of numerous pedestrians. On community roads, there are often many pedestrians walking in various directions along narrow roadways. When applying VO to such situations, the velocity space may become entirely covered by velocity obstacle regions, leaving no viable velocity options.

The second problem is related to achieving the selected velocity. In VO, the velocity pair v_x , v_y that can reach the goal fastest among velocities not belonging to the velocity obstacle region is chosen. Many mobile robots are equipped with differential drives or omnidirectional wheels, making it relatively easy to achieve the selected velocity. However, in case of automobiles, which mostly adopt front-wheel steering and have longer wheelbases, there are significant constraints on achievable velocities. As a result, there can be a significant difference between the selected velocity and the realized velocity, potentially leading to inappropriate trajectory generation.

The third problem relates to road width. Generally, community roads have narrow roadways, which limits the freedom of path selection. On the other hand, in VO, there are cases where a viable velocity is not selected despite being capable of driving on narrow roads. One reason is that VO approximates both pedestrians and the ego vehicle with circles for collision detection. Since the shape of automobiles often differs significantly in terms of width and length, there can be a significant difference between the actual collision detection and the circle approximation. Additionally, the circular approximation tends to generate avoidance paths that take unnecessarily large avoidance distances from obstacles. As a result, on narrow community roads, there can be situations where no velocity candidates are available.

To address these problems, this study attempts to achieve autonomous driving on community roads by extending the capabilities of VO. The extended method is referred to as VO-drive in this research.

2 METHODS

2.1 VO

VO is a method for motion planning of a robot in a dynamic environment with multiple moving obstacles. In this algorithm, based on the current positions and velocities of the robot and obstacles, the velocity space of the robot that may lead to future collisions is defined as the "velocity obstacle." The positions of the robot and obstacle are presented as **A** and **B**, respectively, and their velocities as $\mathbf{v_A}$ and $\mathbf{v_B}$. The size of the robot and obstacles are approximated by circles circumscribing them. Each radius is presented R_A and R_B , respectively. The circle centered at **B** with a radius of $R_A + R_B$ is defined as the collision circle. In this case, the set of relative velocities $\mathbf{v_{A,B}}$ that would result in a collision between **A** and **B** forms a collision cone $\boldsymbol{CC_{A,B}}$ (Fig. 1).
The collision cone $\boldsymbol{CC_{A,B}}$ is a planar region bounded by two tangents, λ_f and λ_r, from **A** to the collision circle. In this region, the relative velocity $\mathbf{v_{A,B}}$ between the robot and the obstacle would result in a collision. Thus, the region of relative velocities $\mathbf{v_{A,B}}$ that lead to a collision is determined.

Next, the region of robot velocities $\mathbf{v_A}$ that would result in a collision is calculated. The obstacle velocity $\mathbf{v_B}$ is added to each velocity in the collision cone $\boldsymbol{CC_{A,B}}$. This is equivalent to translating $\boldsymbol{CC_{A,B}}$ by the velocity $\mathbf{v_B}$ (Fig. 2). If the robot velocity $\mathbf{v_A}$ lies within this translated collision cone, a collision would occur. Therefore, this translated collision cone is referred as the "velocity obstacle."

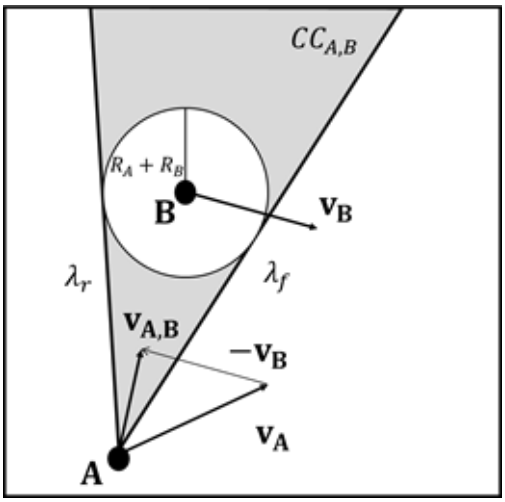

Figure 1 Relative distance $\mathbf{v_{A,B}}$ and collision cone $\boldsymbol{CC_{A,B}}$

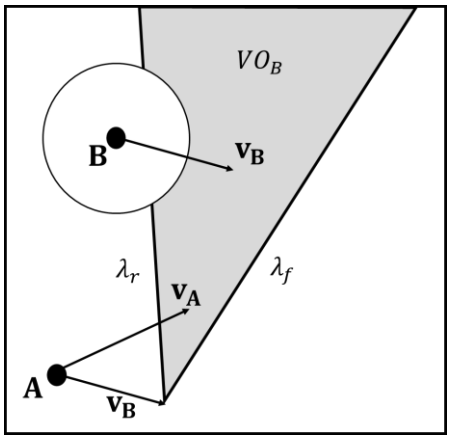

Figure 2 velocity obstacle

The selection of velocity for robot motion is performed as follows. First, an initial velocity is calculated based on a predetermined magnitude of velocity, assuming no obstacles. If the initial velocity lies outside the velocity obstacle, it is directly used for motion. If the initial velocity lies within the velocity obstacle, the velocity closest to the initial velocity on the outside of the velocity obstacle is selected and used for motion.

2.2 VO-Drive

To adapt VO to community roads and autonomous driving, three extensions were made.

2.2.1 Limitation of the Target Object

The first extension addresses the issue of handling a large number of pedestrians. In community roads, there may be many pedestrians walking in various directions along narrow roadways. When applying VO to such a situation, the velocity space is covered by the velocity obstacle region, and no available velocities become exist. To resolve this, a method can be considered to limit the pedestrians (obstacles) that need to be avoided using some criteria. Possible criteria include distance, direction, etc. In this study, a two-Dimensional Time To Collision (2D TTC) based on the time margin until collision is used [11]. It is known that 2D TTC is related to pedestrians' sense of safety in collision avoidance for mobile robots. Therefore, pedestrians with a 2D TTC value above a certain threshold can be considered to have a lower risk of collision and can be excluded from collision detection.

Time To Collision (TTC) is a physical indicator used in Autonomous Emergency Braking (AEB) systems in vehicles. This indicator represents the time until collision with a leading vehicle if the current relative velocity between the ego vehicle and the leading vehicle is maintained. In the world coordinate system, the ego vehicle's front-end position and velocity are presented as x_e and v_e, respectively, while the leading vehicle's rear-end position and velocity are presented as x_l and v_l, respectively. In this case, the relative distance, d_x, and relative velocity, v_x, between the host vehicle and the leading vehicle can be calculated as $x_l - x_e$ and $v_l - v_e$, respectively (Fig. 3).

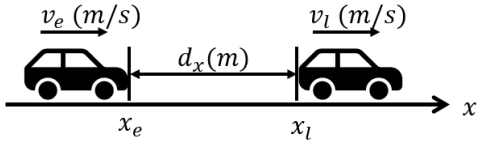

Figure 3 TTC outline figure

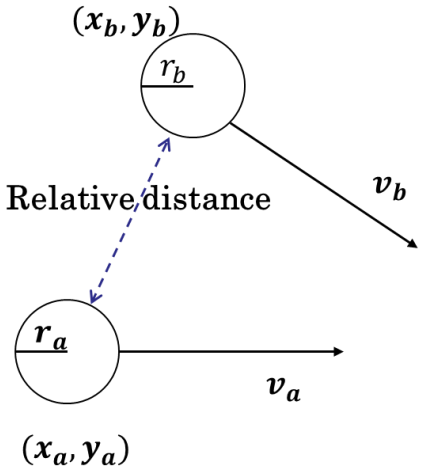

Figure 4 2D TTC outline figure

Therefore, the value of TTC, presented as t_x, can be expressed by the following equation (1).

$$t_x = -\frac{d_x}{v_x} = -\frac{x_l - x_e}{v_l - v_e} \tag{1}$$

In this study, the 2D extension of TTC, referred to as 2D TTC was used. This index takes into account the positional relationship in a 2D space considering the vehicle's longitudinal direction (x-axis in the vehicle coordinate system) and lateral direction (y-axis in the vehicle coordinate system), whereas the previous TTC was calculated based on the positional relationship along the vehicle's longitudinal direction (x-axis) only. In the world coordinate system, the position of the ego vehicle is represented as (x_a, y_a), the position of the obstacle is represented as (x_b, y_b), the velocity of the ego vehicle is presented as (v_{ax}, v_{ay}), the velocity of the obstacle is presented as (v_{bx}, v_{by}), the size of the ego vehicle is presented as r_a, and the size of the obstacle is presented as r_b. Therefore, the relative distance is calculated as $\sqrt{(x_b - x_a)^2 + (y_b - y_a)^2}$, and the relative velocity is calculated as $\sqrt{(v_{bx} - v_{ax})^2 + \left(v_{by} - v_{ay}\right)^2}$ (Fig. 4). Therefore, the value of the 2D TTC is given by the following equation (2).

$$TTC_{2d} = \frac{\sqrt{(x_b - x_a)^2 + (y_b - y_a)^2} - (r_a + r_b)}{\sqrt{(v_{bx} - v_{ax})^2 + \left(v_{by} - v_{ay}\right)^2}} \tag{2}$$

Pedestrians with a 2D TTC value equal to or greater than a certain threshold are considered not requiring avoidance and are therefore excluded from the velocity obstacle calculations.

2.2.2 Velocity Selection Based on Vehicle Motion Constraints

The second point is addressing vehicle motion constraints. Unlike mobile robots, automobiles have significant motion constraints, so an extension was made to select velocities achievable by car steering.

First, assuming the vehicle is either moving straight or performing a steady-state circular motion, the trajectory is calculated [12]. The illustration of this is shown in the figure below (Fig. 5). Let θ be the angle between the X-axis and the vehicle's longitudinal direction (yaw angle), β be the angle between the vehicle's direction of travel and its longitudinal direction (slip angle), r be the angle between the X-axis and the vehicle's direction of travel, and V be the vehicle's velocity. The slip angle is determined by Equation (3), and the angle between the X-axis and the vehicle's direction of travel is given by Equation (4).

$$\beta = \left(\frac{1-\frac{m}{2l}\frac{l_f}{l_r K_r}V^2}{1-\frac{m}{2l^2}\frac{l_f K_f l_r K_r}{K_f K_r}V^2}\right)\frac{l_r}{l}\delta \tag{3}$$

$$r = \left(\frac{1}{1-\frac{m}{2l^2}\frac{l_f K_f - l_r K_r}{K_f K_r}V^2}\right)\frac{V}{l}\delta \tag{4}$$

Therefore, the trajectory of the moving vehicle's center of gravity is considered. The positions and velocities of the vehicle and the obstacle in the world coordinate system are shown in the figure below (Fig. 6). Let (x_e, y_e) and (v_{ex}, v_{ey}) represent the position and velocity of the vehicle, respectively, and (x_p, y_p) and (v_{px}, v_{py}) represent the position and velocity of the obstacle. The obstacle is assumed to move in a straight line at a constant speed, and its trajectory is predicted.

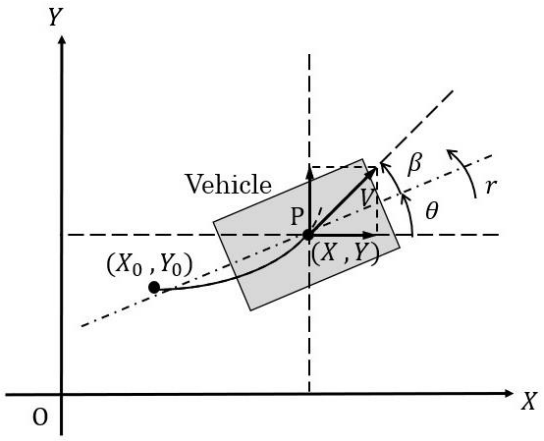

Figure 5 Vehicle trajectory prediction

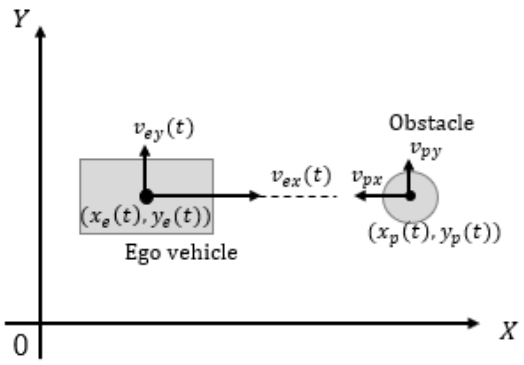

Figure 6 Each variable in the world coordinate system

Given the initial position (X_0, Y_0) and the initial yaw angle θ_0, the position (X, Y) and the yaw angle θ at any given time t can be calculated using equations (5), (6), and (7).

$$X = X_0 + V\int_0^t \cos(\beta+\theta)\,dt \tag{5}$$

$$Y = Y_0 + V\int_0^t \sin(\beta+\theta)\,dt \tag{6}$$

$$\theta = \theta_0 + \int_0^t r dt \tag{7}$$

The actual calculation process is outlined below.

Step1 Provide steering angle for ego vehicle.

Step2 Calculate β and r using the steering angle from Step1 according to equations (3) and (4).

Step3 Using equations (5) and (6) from Step2, calculate the reachable points.

Step4 Calculate the velocity required to reach the speed in Step3.

Step5 Convert the velocity in Step4 to the velocity within the VOmap.

Step6 Prepare a map similar to VOmap, and substitute the value of the steering angle at the velocity position in Step5.

Step7 Repeat Step 1 to 6.

Here is the outline of trajectory prediction (Fig. 7).

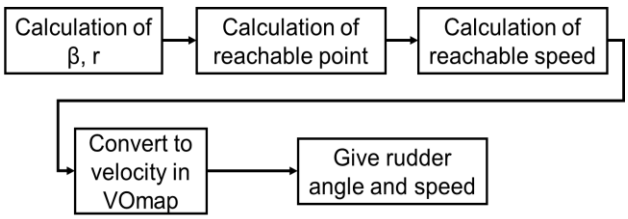

Figure 7 Outline of trajectory prediction

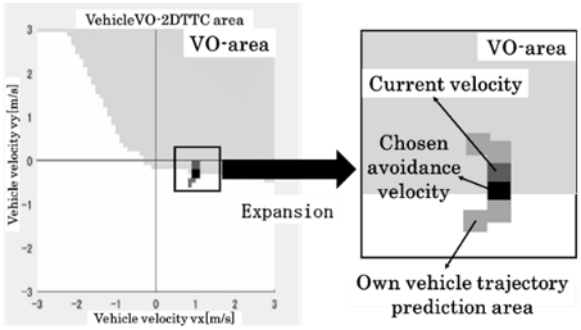

Figure 8 Example of trajectory prediction

However, there is a difference when combining the VO method with trajectory prediction. VO assumes both the ego vehicle and the obstacles move in constant linear motion and generate avoidance paths based on the assumption that the current velocity will continue. On the other hand, trajectory prediction for constant circular motion involves nonlinear motion with constant translational and rotational velocities, making it incompatible to directly apply the VO method.

Therefore, in this case, an attainment point based on the current velocity that would result in a constant circular motion was assumed. The line connecting the starting point and the attainment point was approximated.

The generated trajectory prediction points for the ego vehicle are shown in the figure below (Fig. 8).

2.2.3 Collision Detection Based on the Vehicle Contour

The third point addresses the issue of narrow road widths. In the VO approach, both pedestrians and ego vehicles are approximated as circles for collision detection. However, this approximation can result in significant differences between the actual collision detection and the circle approximation. Using circular approximation often leads to unnecessarily large avoidance routes.

According to the Japanese Cabinet Office, a "community road width" is defined as a road with a carriageway width of less than 5.5 meters in urban areas. If the avoidance route is too large, there is a risk of veering off the road or even the possibility of being unable to avoid the obstacle altogether. To achieve a compact and safe avoidance route, a collision detection method that takes into account the vehicle's contour was adopted (Fig. 9).

By utilizing the vehicle's contour, performing VO calculations from the four corners of the vehicle to the obstacles. Figure 10 shows velocity obstacle area. The original VO area is shown in gray and extended method area shown in black. This shows that it can be observed that extended method results in a smaller area compared to the original method. This approach allows for more precise collision detection and avoidance planning, taking into account the actual shape and size of the vehicle.

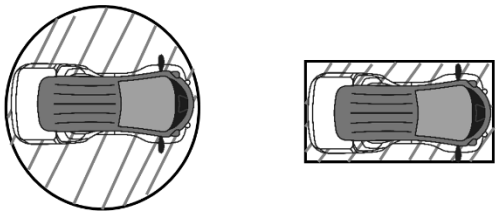

Figure 9 Comparison between circle approximation and contour-based methods

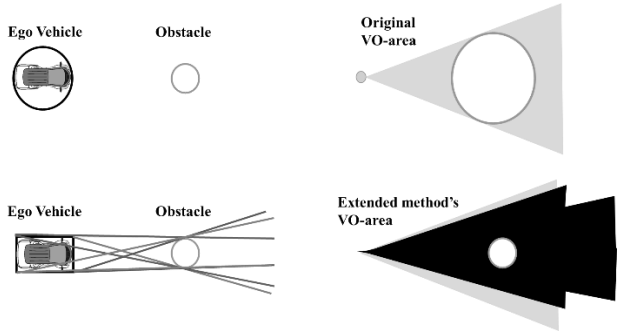

Figure 10 Caomparison of calculation methods between original VO and extended method

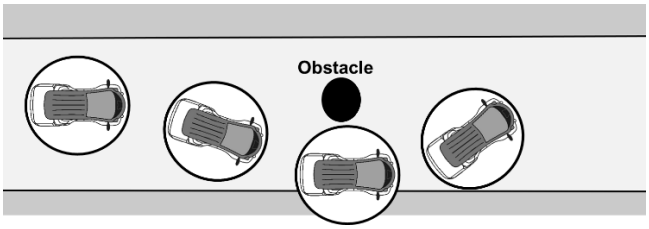

Figure 11 Example of avoidance using circle approximation

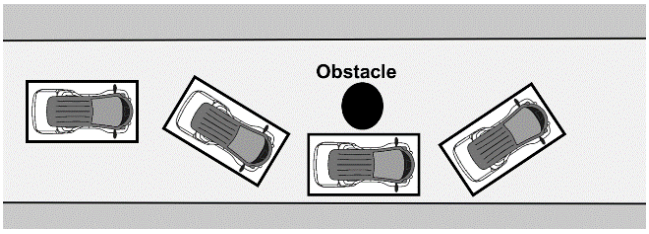

Figure 12 Example of avoidance using vehicle contour

When actually performing circular approximation in a scenario simulating a community road environment, as shown in Fig. 11, attempting to avoid obstacles leads to deviating from the lane due to the constraints of the road width. Therefore, by performing calculations from the four corners of the vehicle, it becomes possible to avoid obstacles while staying within the lane width, as shown in Fig. 12. This approach ensures that the vehicle navigates safely within the available space and minimizes the risk of deviating off the road.

3 SIMULATION EXPERIMENT AND RESULTS

3.1 Experimental Conditions

Using the VO-drive method proposed in this study, a simulation experiment was conducted to compare it with the original VO (Velocity Obstacle) method, DWA (Dynamic Window Approach), and the risk potential method.

The simulation was performed using MATLAB. A time step of 0.1 seconds was used, and the initial value of the vehicle speed was set to 15 km/h. When the path generation method instructed a specific speed, it followed the generated speed by each route generation accordingly.

About the risk potential method, only the repulsive potential from obstacles was defined [13]. The repulsive potential was calculated by the distance from the surface of obstacle. Here, $P_{repulsive}$ shows repulsive potential energy, K_{rep} shows repulsion coefficient, and $distance_{ob}$ shows distance to the obstacle. The expression for the repulsive potential energy is given as Equation 8.

$$P_{repulsive} = \sum \left(\frac{K_{rep}}{distance_{ob}} \right) \tag{8}$$

When TTC falls below 6 seconds, the route is generated to select areas with lowest potential.

DWA (Dynamic Window Approach) requires the setting of three weights: goal direction weight, obstacle distance weight, and velocity weight. In this experiment, these weights were set to 0.1, 0.2, and 0.3, respectively.

For VO-drive, the threshold for 2D TTC was set to 6 seconds as a limitation condition for the target obstacle. Only obstacles with TTC values below this threshold are considered for avoidance. And, the attainment point was defined as the point reachable 0.1 seconds later. For obstacle behavior prediction, the walking speed of the tracked obstacle was calculated using a Kalman filter, and the predicted position was calculated based on the calculated walking speed [14].

3.2 Comparison Between VO-Drive and VO

First, a comparison was conducted between the original VO and the extended VO-drive to confirm the effectiveness of the extension.

A comparative experiment was conducted on the limitation of the target obstacle. The results are shown in Fig. 13. The ego vehicle starts from the position (-15,0) in the world coordinate system and moves straight at a speed of 15 km/h. An experimental scenario was designed where the vehicle needs to avoid a stationary obstacle located at (15,0). From Fig. 13, it can be observed that the extended VO-drive leads to a delay in the timing of avoidance initiation. Conventional VO begins avoidance from the start point, whereas the extended VO-drive proceeds straight initially due to the absence of collision risk and begins avoidance only upon detecting a potential collision danger.

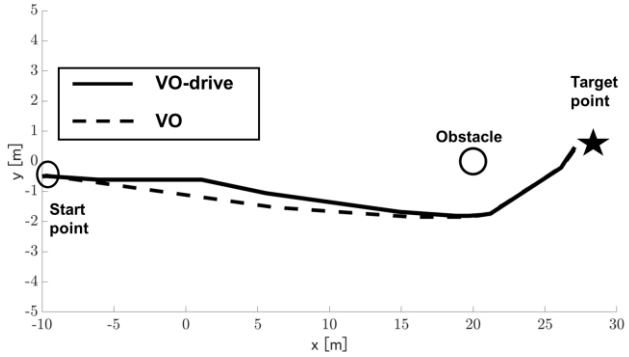

Figure 13 Comparison of target obstacle limitation

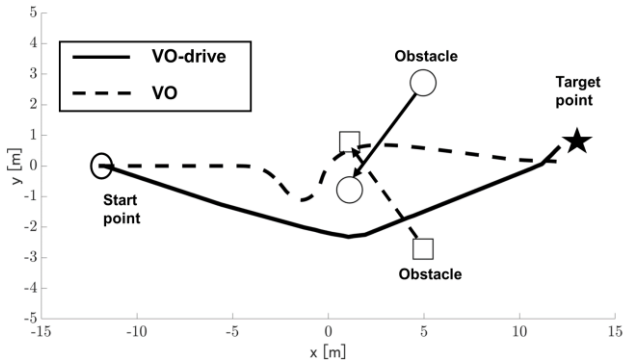

Figure 14 Comparison of vehicle motion constraints

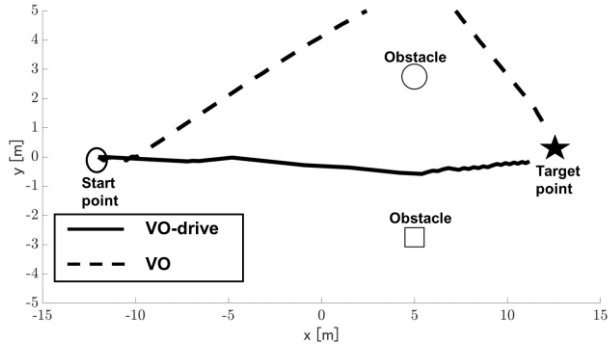

Figure 15 Comparison of collision detection

Second, a comparative experiment was conducted on velocity selection based on vehicle motion constraints. The results are shown in Fig. 14. The ego vehicle starts from the position (-12,0) in the world coordinate system and moves straight at a speed of 15 km/h. Two obstacles are introduced, each moving diagonally at a speed of 0.5 m/s, creating a crossing scenario. From Fig. 14, it can be observed that the proposed method achieves smoother and more efficient avoidance, while the original VO approach exhibits sharp turns.

Lastly, a comparative experiment was then conducted on collision detection based on the vehicle contour. The results are shown in Fig. 15. The ego vehicle starts from the position (-12,0) in the world coordinate system and moves straight at a speed of 15 km/h, aiming to compare whether it can navigate between the obstacles. From Fig. 15, it can be observed that the conventional circle approximation method fails to navigate between the obstacles and takes a significantly larger avoidance path, while the extension allows the vehicle to pass between the obstacles successfully.

3.3 Comparison of VO-Drive and Other Methods

Then, a comparison was made between the proposed VO-drive method and the original VO, DWA, and risk potential method. The horizontal lines shown in the figure represent the width of the community roads, with the width between the upper and lower lines being 5.5m. The experiment scenario was the same as described earlier, with two diagonal-crossing obstacles. In the figures, the distance traveled by each method is shown at the same elapsed time as the progress of the VO-drive method. The elapsed time in the experiment was 23 seconds. The results are shown in Fig. 16. From Fig. 16, it can be observed that the VO-drive method has traveled the farthest within the same elapsed time. The original VO method exhibits similar behavior as in Fig. 14. DWA shows larger avoidance routes compared to the VO-drive method. The risk potential method failed to avoid and came to a stop.

The final generated trajectories are shown in Fig. 17. The elapsed time and maximum avoidance amount for each method until reaching the target point are shown in Table 1. It is evident that the proposed method, VO-drive, achieves the shortest time and maintains avoidance within the road width. VO achieves avoidance with some margin to the road width but takes longer to avoid. DWA avoids by a larger margin than the road width. Regarding the risk potential method, it failed to avoid the obstacle, resulting in a collision after 17 seconds.

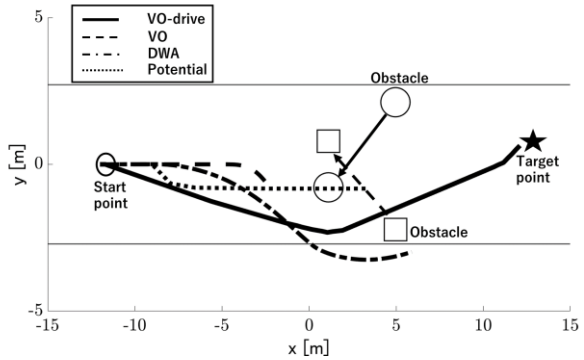

Figure 16 Trajectories of each method at 23 seconds elapsed

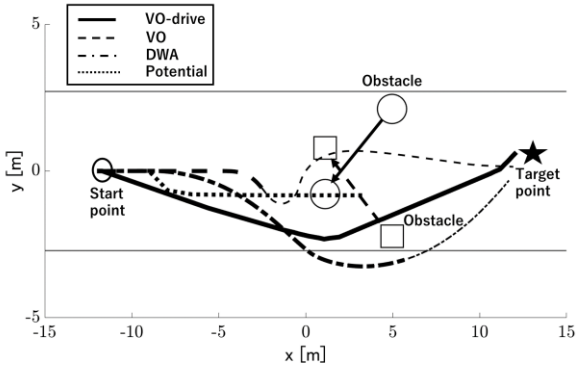

Figure 17 The generated trajectories in the end

Table 1 Comparison of results for each method

	The elapsed time (s)	The maximum avoidance amount (m)
VO-drive	23	2.32
VO	38	0.572
DWA	31	3.25
Risk Potential	NA (fail)	0.826

Based on the results and analysis, it can be concluded that a suitable avoidance method for vehicles and community roads can be proposed by comparing the original approach with the extended one.

4 CONCLUSIONS

By conducting a comparison of methods using simulations, it was possible to demonstrate the usefulness of the proposed VO-drive approach for autonomous driving on urban roads. After conducting simulations, actual experiments were carried out using a vehicle, and successful avoidance routes were performed.

Three research problems were examined. For the first problem, “many pedestrians are present on community roads”, 2D TTC was used to limit pedestrians performing avoidance in “limitation of the target object” of extension 1. From Fig. 13, it was observed that this limitation delays the avoidance timing, suggesting that avoidance can be performed even in congested situations. For the second problem, the difference between the motion of vehicles and robots, the vehicle dynamics of vehicles were applied in extension 2. This allowed the transition from the conventional two-wheeled model to be restricted to the motion of vehicles. For the third problem, the narrow road width, calculations using the vehicle’s four contour instead of the conventional circular approximation were adopted in extension 3. As shown in Fig. 15, using the vehicle’s contour demonstrated that it is possible to pass through the shortest path without large avoidance maneuvers. This suggests that avoidance can be performed even on narrow roads such as community roads.

5 FUTURE WORKS

Currently, the real vehicle experiments are still ongoing. In the future, it is plan to conduct real vehicle experiments, increasing the vehicle's speed and introducing moving obstacles to create an environment closer to real-life urban road conditions. In addition, by having pedestrians actually walk, it is aim to realize avoidance that makes them feel safe.

Finally, the remaining problem for the practical use of the proposed method are discussed. In the second extension, vehicle motion constraints were considered. However, since the avoidance speed determined here was linearly approximated, the motion was not fully accounted for. Actual vehicle motion is nonlinear. Therefore, it is planned to address this issue by using the bicycle model and conducted real vehicle experiments to perform model identification.

APPENDIX

When calculating the VO region, a comparison will be made between the conventional method of circular approximation and the method proposed in this paper, which uses the vehicle's corner points. In contrast to square robots, vehicles have a rectangular shape. Therefore, when approximating with a circle, unnecessary parts may emerge (refer to Fig. 9). Performing circular approximation on narrow roads, such as community roads, in this state may not provide sufficient space for obstacle avoidance, or there is a risk of avoiding obstacles largely. Therefore, by conducting an approximation from the four corners of the vehicle, it is believed that even large vehicles like cars can navigate narrow roads like community roads while avoiding obstacles. Vehicle corner approximation is shown in Fig. 10.

The discussion will consider simplified shapes of "vertical bar" and "horizontal bar," and subsequently extend to rectangular shapes resembling vehicles.

To begin, it will be examined the case where a vertical bar, representing a simplified shape, is moving and encountering an obstacle of a certain size. The length of the vertical bar in Fig. 18 is taken as $2 \times r_1$, and the obstacle is approximated as a circle with a radius of r_1.

In this scenario, considering that the top and bottom two points of the vertical bar can move as individual points, the resulting VO region can be depicted as shown in Fig. 19.

As the bar is rigid, the top and bottom endpoints cannot move independently. To translate this scenario into one where the velocity obstacle is defined with respect to the center point of the bar, the VO region generated from these two points is shifted to the center of the vertical bar. These two regions, VO_a and VO_b, become the velocity obstacle regions where the endpoints of the bar would collide as it moves. As all points between the top and bottom endpoints lie within the bar, the combined VO_v region encompassing VO_a and VO_b becomes the velocity obstacle region for the entire bar's movement. In this case, the distance from the obstacle to the boundary of the VO_v region is $r_1 + r_2$, where r_1 represents the radius of the vertical bar and r_2 represents the radius of the obstacle (Fig. 20). This is equal to the conventional VO calculation method using circular approximation.

Next, it will be considered a similar analysis for the horizontal bar scenario in Fig. 21.

In this scenario, generating the VO region from two points on the left and right results in the configuration shown in Fig. 22.

Similarly, shift the VO region generated from the two points on the left and right to the center of the horizontal bar. This is illustrated in Fig. 23.

At this point, it becomes evident that the distance from the shifted VO region to the obstacle is shorter than $r_1 + r_2$. This suggests that when approximating with a horizontal bar, the size of the VO region might be smaller compared to the conventional VO calculation method. Let's now verify how much smaller the size of the VO region becomes when compared to the traditional VO calculation method (Fig. 24).

Figure 18 Scenario of vertical bar approximation

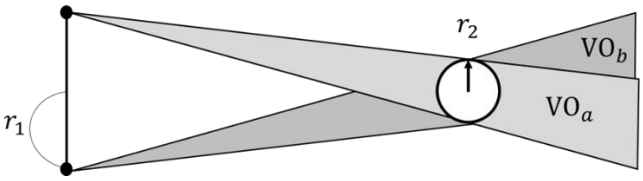

Figure 19 Generation of VO region using vertical bar approximation

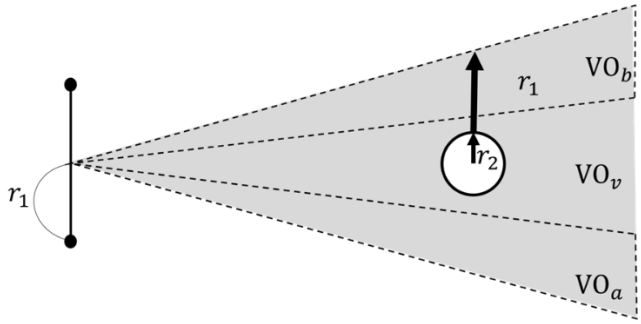

Figure 20 Shifting the VO region to the center of the vertical bar approximation

Figure 21 Scenario of horizontal bar approximation

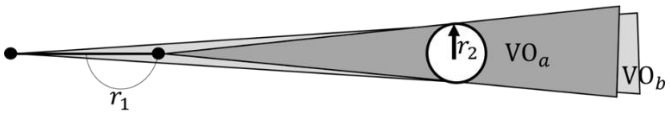

Figure 22 Generation of VO region using horizontal bar approximation

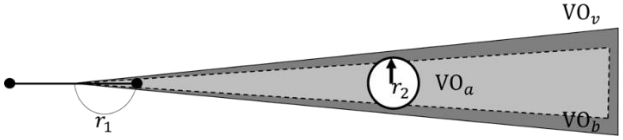

Figure 23 Shifting the VO region to the center of the horizontal bar approximation

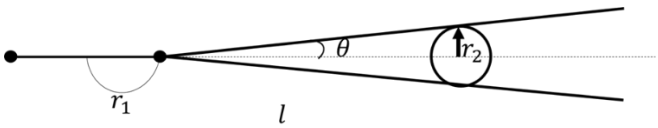

Figure 24 Calculation $\boldsymbol{\theta}$ from the right point of the horizontal bar approximation

Considering the VO region from the right point when approximated by a horizontal bar, as shown in Fig. 24. Here, the angle θ can be expressed as Equation 9.

$$\theta = \tan^{-1}\frac{r_2}{l - r_1} \tag{9}$$

Here, it will be examined how much the VO region generated from the right side of the horizontal bar increases when shifted to the center of the bar (Fig. 25).

Here, when considering the difference $\boldsymbol{d}$ between the VO regions before and after the shift, it can be expressed as Equation 10.

$$d = l \cdot \tan\left(\tan^{-1}\frac{r_2}{l - r_1}\right) - r_2 \tag{10}$$

If the calculated value of $\boldsymbol{d}$ obtained here is shorter than $\boldsymbol{r_1}$, it becomes evident that the resulting VO region will be smaller than the conventional VO region.

Finally, it will be considered the calculations from the corners of the vehicle. It will examine a scenario depicted in Fig. 26.

As mentioned earlier, it has been established that the vertical bar approximation results consistent with the conventional VO method, while the horizontal bar approximation leads to a smaller VO region compared to the traditional method. Based on this, the approach is to calculate the velocity obstacle region in the width direction of the vehicle using conventional circular approximation and then combine this region with the velocity obstacle region in the length direction of the vehicle using a similar method as the horizontal bar approximation (Fig. 27). This way, the overall velocity obstacle region for the entire vehicle can be determined.

For this scenario, the generated VO regions are shown in Fig. 28.

Upon shifting the generated VO regions to the center of the horizontal bar, they transform as shown in Fig. 29.

In this context, the modification in size due to the displacement of the VO regions will be examined.

For the angle θ shown in Fig. 30, it can be expressed Equation 11.

$$\theta = \tan^{-1}\frac{r_1 + r_2}{l - r_1} \tag{11}$$

Subsequently, the difference d between the VO regions before and after the shift, it can be expressed as Equation 12.

$$d = l \cdot \tan\left(\tan^{-1}\frac{r_1 + r_2}{l - r_1}\right) - (r_1 + r_2) \tag{12}$$

Here, a comparison between the proposed method and the conventional circular approximation is conducted. As a method of comparison, the radius of the extended circle from the conventional VO calculation method and the value $d + (r_1 + r_2)$ from the current approach are contrasted. Since the value depends on the distance l from the center of the vehicle

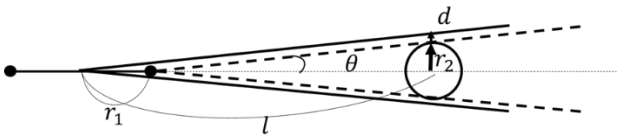

Figure 25 Calculation $\boldsymbol{\theta}$ and $\boldsymbol{d}$ from the center of the horizontal bar approximation

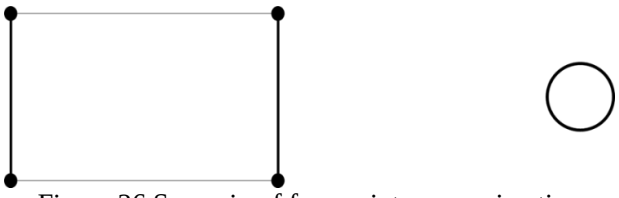

Figure 26 Scenario of four points approximation

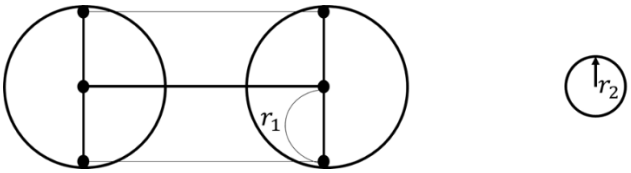

Figure 27 Suggest method to generate VO region

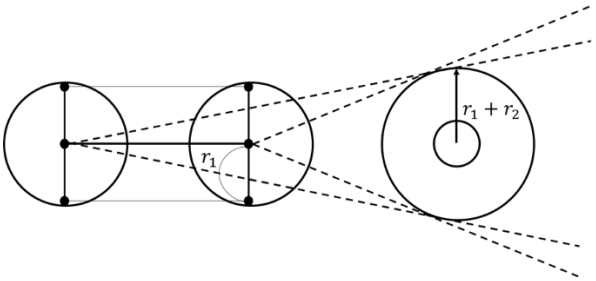

Figure 28 Generation of VO region from suggest method

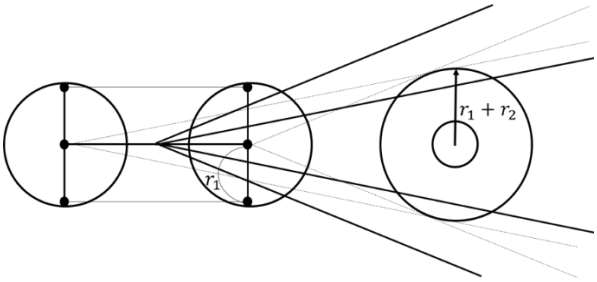

Figure 29 Shifting VO region to the center of the four points approximation

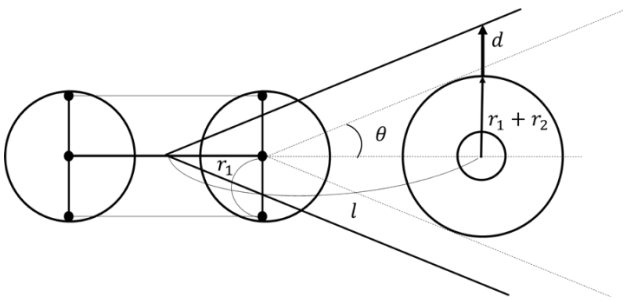

Figure 30 Calculation $\boldsymbol{\theta}$ and $\boldsymbol{d}$ from the center of the four points approximation

to the center of the obstacle, the comparison was carried out by varying the value of l. The radius of the host vehicle r_1 is set to 0.75 m, and the radius of the obstacle r_2 is set to 0.5 m. For simplicity, consider the length of the vehicle as being twice its width. As a result, it was found that for distance less than 1 to 4.9 meters, the conventional circular approximation yields a smaller generated VO region, whereas for distance greater than 4.9 meters, the proposed method leads to a smaller VO region.

So far, assumptions have been made regarding vehicles performing only parallel movements. However, in reality, vehicles not only engage in parallel movements but can also involve rotational motion during navigation. Therefore, navigation in dynamic environments for robots like cars has been developed by David Wilkie and others [15]. The paper introduces the concept of generalized velocity obstacles, aiming to address challenges when utilizing velocity obstacles with kinematically constrained agents such as car-like robots. The formulation is expressed as follows:

$$VO_{(A|B)} = \{\mathrm{v}|\exists t > 0 :: \|A(t,u) - B(t)\| < r_A + r_B \} \quad (13)$$

$$u = arg \min_{u' \notin \cup_{B_i} VO_{(A|B_i)}} \|u^* - u'\| \quad (14)$$

However, because analytical solutions were not feasible, experiments were conducted through simulations. Specifically, additional simulations were conducted to examine the differences in trajectories when the vehicle performs circular evasion around obstacles. In this scenario, the vehicle travels straight from the Start point to the Target point at a speed of 15 km/h, avoiding obstacles. The size of the vehicle in VO-drive simulations was set at a width of 1.5m and a length of 2.13m, and experiments were performed with a radius of 1.357m during VO scenarios. The experiments started with a distance of 25m between the vehicle and the obstacle. For the simulation comparison of differences due to vehicle approximation, 2D TTC was set to 6 seconds for both VO-drive and VO, and self-vehicle trajectory prediction was applied to both. Figure 31 shows the results of the simulation. The upper and lower lines in Fig. 31 represent the road width, set at 5.5m to simulate a community road. As evident from the figure, the proposed method can avoid obstacles while staying within the vehicle width. In contrast, with the conventional circular approximation, it is clear that avoiding within the vehicle width is not achieved. Consequently, it can be inferred that the proposed method performs better in narrow road scenarios when following a straight trajectory.

VO-drive, in contrast to the conventional VO, differs in computational complexity. While the conventional method performs VO calculations from the center of the vehicle, the proposed method calculates VO from the four corners of the vehicle. As a result, the computational complexity of the proposed method is expected to be four times higher than that of the conventional method.

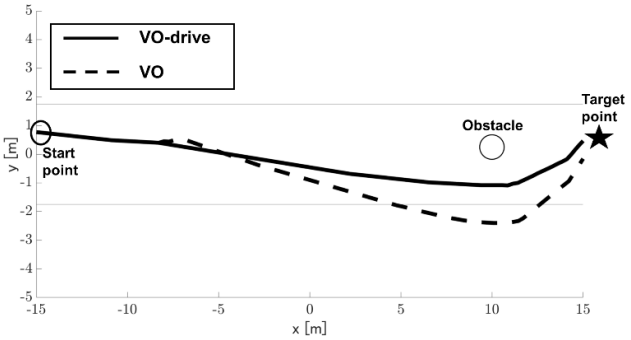

Figure 31 Differences in trajectory by vehicle approximation

It should be noted that the proposed method mentioned above only accounts for parallel displacement. Future work needs to include considerations for rotational movement as well.

REFERENCES

[1] Ministry of Land, Infrastructure, Transport and Tourism, Community road traffic safety measures portal, https://www.mlit.go.jp/road/road/traffic/sesaku/anzen.html.

[2] D. Fox, W. Burgard, S. Thrun, “The dynamic window approach to collision avoidance,” IEEE Robot. Autom. Mag., vol. 4, no. 1, pp. 23-33 (1997).

[3] M. T. Wolf, J. W. Burdick, “Artificial Potential Functions for Highway Driving with Collision Avoidance”, IEEE International Conference on Robotics and Automation (2008).

[4] R. Akabane, Y. Kato, “Pedestrian Trajectory Prediction Based on Transfer Learning for Human-Following Mobile Robots”, IEEE Access, vol. 9, pp. 126172-126185 (2021).

[5] A. J. Sathyamoorthy, U. Patel, T. Guan, D. Manocha, “Frozone: Freezing-Free, Pedestrian-Friendly Navigation in Human Crowds”, IEEE Robot. Automat. Lett., vol. 5, no.3, pp.4352-4359 (2020).

[6] P. Fiorini, Z. Shiller, “Motion Planning in Dynamic Environments Using Velocity Obstacles”, The International Journal of Robotics Research, vol.17, no.7, pp.760-772 (1998).

[7] J. v. d. Berg, M. Lin, D. Manocha, “Reciprocal Velocity Obstacles for Real-Time Multi-Agent Navigation”, IEEE International Conference on Robotics and Automation, pp. 1928-1935 (2008).

[8] J. v. d. Berg, Stephen J, Guy, M. Lin, D. Manocha, “Optimal Reciprocal Collision Avoidance for Multi-Agent Navigation”, IEEE International Conference on Robotics and Automation, pp. 1928-1935 (2010).

[9] M. Gu, Y. Huang, “Dynamic Obstacle Avoidance of Mobile Robot Based on Adaptive Velocity Obstacle”, 36th Youth Academic Annual Conference of Chinese Association of Automation (YAC), pp. 776-781 (2021).

[10] J. D. Jeon, B. H. Lee, “Ellipse-based velocity obstacles for local navigation of holonomic mobile robot”, Electronics Letters, vol. 50, no. 18, pp. 1279-1281 (2014).

[11] Y. Yada, S. Michita, S. Komiya, T. Wakita, “Pedestrian Cooperative Autonomous Mobility -Path Planning Adapted to Pedestrian Face Direction-”, International

Journal of Informatics Society, Vol. 15, No. 1, pp. 43-51 (2023).
[12] M. Abe, Automotive Vehicle Dynamics Trajectory and Applications, Tokyo Denki University Press (2012).
[13] S. Michita, “Autonomous Driving on Community Roads Using Small Mobility – study on Safe Stop Decision –, Kanagawa Institute of Technology, Master’s Thesis (2023).
[14] T. Goto, “Pedestrian behavior prediction and forecast circle generation using Kalman filter”, Kanagawa Institute of Technology, Undergraduate Thesis (2019).
[15] D. Wilkie, J. v. d. Berg, D. Manocha, “Generalized Velocity Obstacles”, IEEE/RSJ International Conference on Intelligent Robots and Systems, pp. 5573-5578 (2009).
(Received: December 15, 2023)
(Accepted: August 22, 2024)

Takumi Seita
He was graduated from school of Vehicle System Engineering, Kanagawa Institute of Technology as a bachelor. Also, he is a master student at Graduate School of Mechanical system engineering, Kanagawa Institute of Technology, Japan. His expertise is development of Autonomous Mobility.

Shunsuke Michita
He was graduated from school of Vehicle System Engineering, Kanagawa Institute of Technology as a bachelor. Also, he earned his master's degree in the Department of Mechanical System Engineering from the Kanagawa Institute of Technology. He is currently employed at Honda Motor Co., Ltd.

Seiji Komiya
He was graduated from the Graduate School of Engineering, Yokohama National University in March 1990. Joined Kanagawa Institute of Technology, where he currently works. His expertise is the development of intelligent mobility.

Toshihiro Wakita received B.E. from Kyoto University, M.S. from The University of Tokyo and Ph.D. degree from Nagoya University in 1983, 1985 and 2006, respectively. He is currently a professor at Kanagawa Institute of Technology. His research interest includes intelligent mobility and human machine interface. He is a member of IEEE, IEICE, and IPSJ.